

## Atropisomerism

## Catalytic and Enantioselective Control of the C–N Stereogenic Axis via the Pictet–Spengler Reaction

Ahreum Kim<sup>†</sup>, Aram Kim<sup>†</sup>, Sunjung Park, Sangji Kim, Hongil Jo, Kang Min Ok, Sang Kook Lee, Jayoung Song, and Yongseok Kwon\*

**Abstract:** An unprecedented example of a chiral phosphoric acid-catalyzed atroposelective Pictet–Spengler reaction of *N*-arylindoles is reported. Highly enantioenriched *N*-aryl-tetrahydro- $\beta$ -carbolines with C–N bond axial chirality are obtained via dynamic kinetic resolution. The hydrogen bond donor introduced on the bottom aromatic ring, forming a secondary interaction with the phosphoryl oxygen, is essential to achieving high enantioselectivity. A wide variety of substituents are tolerable with this transformation to provide up to 98% ee. The application of electron-withdrawing group-substituted benzaldehydes enables the control of both axial and point stereogenicity. Biological evaluation of this new and unique scaffold shows promising antiproliferative activity and emphasizes the significance of atroposelective synthesis.

Asymmetric catalysis has paved new ground in the preparation of chiral molecules containing a stereogenic axis by enabling noncovalent interactions between substrates and catalysts.<sup>[1]</sup> In particular, much interest has been focused on the control of axial chirality around a C–C bond, which has led to many valuable methods over the past decade.<sup>[2]</sup> However, atropisomerism around a C–N bond in biaryls has received relatively less attention,<sup>[3,4]</sup> even though nitrogen-containing heterocycles are considered biologically relevant scaffolds.<sup>[5]</sup>

$\beta$ -Carbolines and tetrahydro- $\beta$ -carbolines are of widespread interest because of their natural abundance and various biological activities (Figure 1a).<sup>[6]</sup> Because of their intriguing biological and physicochemical properties, synthetic efforts have been made to efficiently construct this scaffold.<sup>[7]</sup> Because of the ubiquitous indole precursor, the formation of the C ring (Figure 1b) frequently allows more straightforward synthetic approaches.<sup>[7,8]</sup> Given the dense substitutions at the *N*-9 position, biaryl frameworks such as *N*-aryl- $\beta$ -carboline are expected to have C–N axial chirality.

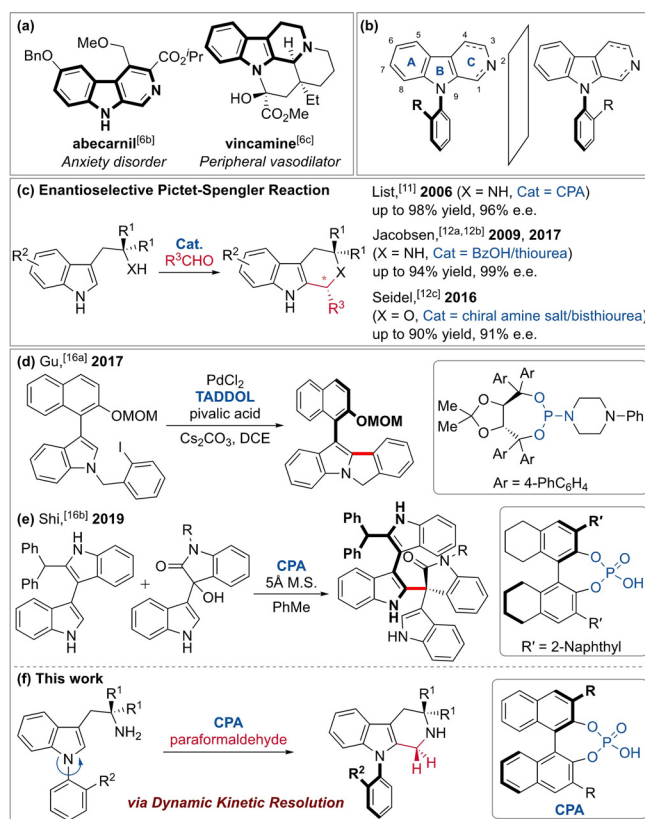


**Figure 1.** a) Biologically active  $\beta$ -carbolines. b) Possible atropisomerism in  $\beta$ -carbolines. c) Enantioselective Pictet–Spengler reactions. d)–f) Atroposelective dynamic kinetic resolution of substituted indoles.

Pictet–Spengler cyclization is an acid-mediated intramolecular Friedel–Craft type reaction involving iminium ions.<sup>[9]</sup> It has been widely used to synthesize complex natural products, including  $\beta$ -carboline alkaloids.<sup>[10]</sup> Since the List group developed an asymmetric Pictet–Spengler reaction of indoles using a catalytic chiral phosphoric acid,<sup>[11]</sup> a number of asymmetric variants of this transformation have been reported (Figure 1c).<sup>[12]</sup> Inspired by these elegant methodologies, we chose to explore the atroposelective Pictet–Spengler cyclization of *N*-arylindoles. To the best of our knowledge, an atroposelective version of this reaction is unprecedented.

We hypothesized that chiral phosphoric acids<sup>[13,14]</sup> can catalyze cyclization atroposelectively via dynamic kinetic resolution (DKR),<sup>[15]</sup> based on the difference in rotational barriers between the substrate and the cyclized product. The DKR strategy for the atroposelective transformation of 3-arylindole has recently been investigated.<sup>[16]</sup> The Gu group

[\*] A. Kim,<sup>[†]</sup> A. Kim,<sup>[†]</sup> S. Park, S. Kim, H. Jo, Prof. Dr. K. M. Ok, Prof. Dr. Y. Kwon

Department of Chemistry, Sogang University  
35 Baekbeom-ro, Mapo-gu, Seoul (Republic of Korea)  
E-mail: ykwon@sogang.ac.kr

Prof. Dr. S. K. Lee, Dr. J. Song  
College of Pharmacy, Seoul National University  
1 Gwanak-ro, Gwanak-gu, Seoul (Republic of Korea)

[†] These authors contributed equally to this work.

Supporting information and the ORCID identification number(s) for the author(s) of this article can be found under:  
<https://doi.org/10.1002/anie.202100363>.

reported palladium-catalyzed atroposelective intramolecular C–H cyclization using TADDOL as a chiral ligand (Figure 1d).<sup>[16a]</sup> More recently, chiral phosphoric acid-catalyzed atroposelective C-2 functionalization of the 3,3'-bisindole skeleton was reported by the Shi group (Figure 1e).<sup>[16b]</sup> In the report, they suggested that the acidic activation of electrophiles by chiral phosphoric acid and the interaction between the phosphate counterion and NH moiety of indole are crucial because of the bifunctional activation of a chiral phosphoric acid. From this point of view, since the absence of N–H in *N*-arylidole could have a detrimental effect on selectivity, an additional hydrogen bond donor might be required to achieve high selectivity. Herein, we report a highly atroposelective Pictet–Spengler cyclization of *N*-arylidoles catalyzed by a chiral phosphoric acid (Figure 1f).

To test our hypothesis, we designed the initial substrate **1a** in which the *gem*-dimethyl group is introduced to accelerate the transformation by the Thorpe–Ingold effect (Table 1). To avoid any other additional effects by potential point stereogenicity, paraformaldehyde, an unsubstituted aldehyde source, was chosen. The reaction of **1a** with **P1** and paraformaldehyde afforded tetrahydro- $\beta$ -carboline **2a** in high yield, albeit with low enantioselectivity (entry 1). However, completely different results were obtained when the methyl group was replaced with a benzylamino group. To our delight, highly improved selectivity was achieved in the reaction of **1b** (87% *ee*, entry 2). With substrate **1b**, chiral phosphoric acid catalysts have been screened in which the enantioselectivity is highly affected by the substitution

pattern on the aryl ring (*R'* in the Table 1). The reactions of **P2** or **P3** containing *meta*-substituents showed moderate selectivity (entries 3 and 4). Regardless of the electronic or steric factor of the *para*-substituents, poor enantioselectivities were observed (entries 5–7). The anthracenyl-substituted catalyst displayed slightly better selectivity (73% *ee*) than the phenanthryl substituted catalyst (entries 8 vs. 9). Catalyst **P9** with 2,4,6-tricyclohexyl substituents delivered **2b** in the highest observed enantioselectivity under the initial reaction conditions (entry 10). The cyclization of **1b** with VAPOL-type chiral phosphoric acid **P10** produced **2b** with lower enantioselectivity (entry 11). With the optimal catalyst, **P9**, other reaction parameters were evaluated, such as aldehyde source, solvent, temperature and equivalence.<sup>[17]</sup> During the optimizations, slightly higher selectivity was obtained (96% *ee*, **2b** in Table 2), when the reaction was performed at 2 °C.

With the optimal reaction conditions in hand, the substrate scope was examined, as summarized in Table 2.

**Table 2:** Substrate scope.<sup>[a–d]</sup>

Reaction scheme for Table 2: Substrate **1** (with *R*<sup>1</sup>, *R*<sup>2</sup>, *R*<sup>3</sup> substituents) reacts with paraformaldehyde (1.5 equiv) and catalyst **P9** (10 mol%) in PhMe at 2 °C to form product **2** (with *R*<sup>1</sup>, *R*<sup>2</sup>, *R*<sup>3</sup> substituents). *R*<sup>1</sup> = 2,4,6-tricyclohexylphenyl, **P9**.

Entry	Substrate	Catalyst	Yield [%]	<i>ee</i> [%]
1	<b>1a</b> ( <i>R</i> = Me)	<b>P1</b> (( <i>R</i> )–TRIP)	<b>2a</b> , 86	22
2	<b>1b</b> ( <i>R</i> = NHBn)	<b>P1</b> (( <i>R</i> )–TRIP)	<b>2b</b> , 90	87
3	<b>1b</b>	<b>P2</b>	<b>2b</b> , 91	60
4	<b>1b</b>	<b>P3</b>	<b>2b</b> , 86	48
5	<b>1b</b>	<b>P4</b>	<b>2b</b> , 71	6
6	<b>1b</b>	<b>P5</b>	<b>2b</b> , 81	8
7	<b>1b</b>	<b>P6</b>	<b>2b</b> , 82	4
8	<b>1b</b>	<b>P7</b>	<b>2b</b> , 59	66
9	<b>1b</b>	<b>P8</b>	<b>2b</b> , 98	73
10	<b>1b</b>	<b>P9</b>	<b>2b</b> , 99	94
11	<b>1b</b>	<b>P10</b>	<b>2b</b> , 97	12 <sup>[d]</sup>

Chemical structures of catalysts **P1–P9** and **P10** are shown. **P1–P9** are VAPOL-type chiral phosphoric acids with various *R'* substituents. **P10** is a VAPOL-type chiral phosphoric acid with a 2,4,6-tricyclohexylphenyl substituent.

**Table 1:** Catalyst screening.<sup>[a]</sup>

Reaction scheme for Table 1: Substrate **1a** (*R* = Me) or **1b** (*R* = NHBn) reacts with paraformaldehyde (1.5 equiv) and catalyst **P1–P10** (10 mol%) in PhMe at rt, 4–24 h to form product **2a** (*R* = Me) or **2b** (*R* = NHBn).

Entry	Substrate	Catalyst	Yield [%] <sup>[b]</sup>	<i>ee</i> [%] <sup>[c]</sup>
1	<b>1a</b>	<b>P1</b> (( <i>R</i> )–TRIP)	<b>2a</b> , 86	22
2	<b>1b</b>	<b>P1</b> (( <i>R</i> )–TRIP)	<b>2b</b> , 90	87
3	<b>1b</b>	<b>P2</b>	<b>2b</b> , 91	60
4	<b>1b</b>	<b>P3</b>	<b>2b</b> , 86	48
5	<b>1b</b>	<b>P4</b>	<b>2b</b> , 71	6
6	<b>1b</b>	<b>P5</b>	<b>2b</b> , 81	8
7	<b>1b</b>	<b>P6</b>	<b>2b</b> , 82	4
8	<b>1b</b>	<b>P7</b>	<b>2b</b> , 59	66
9	<b>1b</b>	<b>P8</b>	<b>2b</b> , 98	73
10	<b>1b</b>	<b>P9</b>	<b>2b</b> , 99	94
11	<b>1b</b>	<b>P10</b>	<b>2b</b> , 97	12 <sup>[d]</sup>

Chemical structures of catalysts **P1–P9** and **P10** are shown. **P1–P9** are VAPOL-type chiral phosphoric acids with various *R'* substituents. **P10** is a VAPOL-type chiral phosphoric acid with a 2,4,6-tricyclohexylphenyl substituent.

[a] Reaction conditions: **1** (0.050 mmol, 1.0 equiv), paraformaldehyde (0.075 mmol, 1.5 equiv), **P1–P10** (0.005 mmol, 10 mol%), PhMe (0.5 mL, 0.1 M). [b] Isolated yields. [c] Enantiomeric excesses were determined by chiral-phase HPLC analysis. [d] The opposite enantiomer was obtained as a major enantiomer.

[a] Reaction conditions: **1** (0.050 mmol, 1.0 equiv), paraformaldehyde (0.075 mmol, 1.5 equiv), **P9** (0.005 mmol, 10 mol%), PhMe (0.5 mL, 0.1 M). [b] The reported results are the average of two runs. [c] Isolated yields. [d] Enantiomeric ratios were determined using chiral-phase HPLC analysis. [e] The reaction with 1.32 g (3.57 mmol) of **1b** provided **2b** in 95% yield and 96% *ee*. [f] For crystallization, the 4-bromobenzamide derivative was prepared. [g] After the cyclization of **1n** under the standard reaction conditions, the crude product was tosylated in situ.

Initially, different substitution patterns on the bottom arene of the *N*-arylindole moiety were tested. The cyclization of dibenzyl-substituted **1c** with the catalyst **P9** afforded **2c** in only 26% yield with moderate selectivity (56% *ee*). The replacement of the benzylamino group with a methylamino group and benzamide was tolerable under these reaction conditions (for **2d**, 92% *ee*; for **2e**, 97% *ee*). In the reaction of **1f** containing the methyl carbamate, cyclized product **2f** was produced in 67% yield with 76% *ee*. We observed the racemization of **2f** on the bench top, which may cause lower enantioselectivity during the reaction and purification procedures. Then, we examined the substrate bearing additional substituents on the bottom arene ring. Unfortunately, it was observed that **1g** containing a methyl group next to the benzylamine was not tolerable under these reaction conditions (30% *ee*), presumably due to unfavorable steric repulsions with **P9**. Substrates **2h** and **2i** bearing the electron-donating and electron-withdrawing groups, respectively, afforded the desired product in good yield and with excellent enantioselectivity. While the cyclization of **1j** produced **2j** in 96% yield and 98% *ee*, the reaction of *o,o'*-disubstituted substrate **1k** led to a different selectivity depending on the conversion. Although DKR was not carried out due to the steric congestion of **1k**, kinetic resolution still resulted in high selectivity (93% *ee*, see below). The homologated benzylamine substrate, **1l** provided the desired product **2l**, albeit with moderate selectivity (70% *ee*). The substitution of the dimethyl group at tryptamine with cyclohexyl was tolerable to afford **2m** in 85% yield and 96% *ee*. The reaction of the tryptamine derivative **1n** smoothly led to cyclization with high enantioselectivity (94% *ee*). The selectivity was measured after in situ tosylation owing to instability during chromatographic purification of the naked secondary amine. Our catalytic system was effective in 5-substitution of indole with the methoxy and chloride groups (for **2o**, 96% *ee*; for **2p**, 94% *ee*). The reaction can be run on a gram scale (1.32 g of **1b**) without diminishing neither the yield nor the enantioselectivity (95% yield, 96% *ee*). The absolute configuration of **2b** was determined by X-ray crystallography after amidation with *p*-bromobenzoyl chloride.<sup>[17]</sup>

With excellent overall atroposelectivity, we turned our attention to the control of the stereogenic center along with the stereogenic axis. While the control of two different stereogenic element is highly desirable, a limited number of examples have been reported.<sup>[16b,18]</sup> We envisioned that a stereochemically complex setting in this scaffold would be realized by employing substituted aldehydes.<sup>[11,12]</sup> In our first attempts with benzaldehyde, the cyclization of **1b** did not afford the cyclized product even at higher temperature or higher catalyst loading. However, when benzaldehydes bearing an electron-withdrawing group were employed, the reaction afforded the desired products with good to moderate selectivity (Table 3). For example, the reaction of **1b** with *p*-nitrobenzaldehyde at 80°C smoothly afforded **2q** in 9:1 d.r. and >99% *ee*. It was observed that *p*-substitutions such as trifluoromethyl-, cyano-, and methyl ester groups are tolerable (for **2r** and **2s**, 7:1 d.r.; for **2t**, 6:1 d.r.). While the reaction of **1e** with *p*-nitrobenzaldehyde produced **2u**, albeit with

**Table 3:** Substrate scope with benzaldehydes.<sup>[a–c]</sup>

 84% yield, 9:1 d.r., >99% e.e.	 83% yield, 7:1 d.r., >99% e.e.	 84% yield, 7:1 d.r., >99% e.e.
 79% yield, 6:1 d.r., >99% e.e.	 92% yield, 4:1 d.r., >99% e.e.	 98% yield, 10:1 d.r., >99% e.e.

[a] Reaction conditions: **1** (0.050 mmol, 1.0 equiv), aldehyde (0.075 mmol, 1.5 equiv), **P9** (0.010 mmol, 20 mol%), PhMe (0.5 mL, 0.1 M). [b] Isolated yields. [c] Diastereomeric and enantiomeric ratios were determined using chiral-phase HPLC analysis. [d] The relative stereochemistry was confirmed by X-ray crystallography of (±)-**2u**.<sup>[17]</sup>

lower diastereoselectivity, the reaction with *m*-cyanobenzaldehyde produced **2v** in 98% yield and 10:1 d.r.

Based on our data thus far, a putative mechanistic model is proposed, as shown in Figure 2. Condensation of the substrate and paraformaldehyde afforded imine intermediates **I** and *ent*-**I** in dynamic equilibrium. Because we observed the conversion of **1b** to **2b** without the catalyst,<sup>[19]</sup> *ent*-**I** could be transformed to *ent*-**2b**. However, catalyst **P9** could accelerate the cyclization of **I** by forming an iminium-phosphate ion pair and interacting with the phosphate counterion with the amino group.<sup>[14]</sup> This interaction could induce the observed relative stereochemistry in Table 3, in which the iminium ion could approach the benzylamino group in the same plane. The DKR mechanistic pathway can be further supported by the results of **2k**. When the reaction was performed within 12 h, **2k** was obtained in 45% yield and 93% *ee*. However, a longer reaction time (19 h) led to poor selectivity (83% yield, 36% *ee*), which clearly showed the differences between the KR vs. the DKR pathways and the

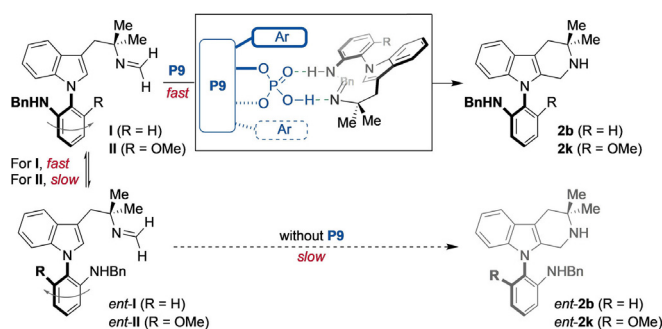


**Figure 2.** Putative reaction mechanism.



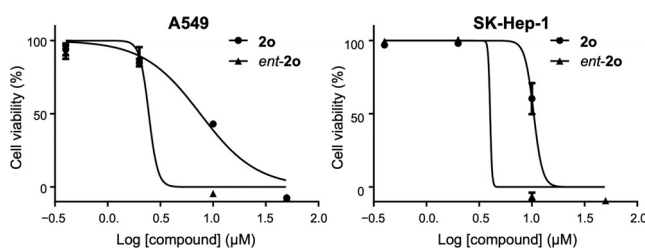
importance of catalytic acceleration to achieve high selectivity compared to the background rate. Further mechanistic studies are currently ongoing in our laboratory.

Given the biological significance of  $\beta$ -carboline derivatives,<sup>[6,7]</sup> especially as potential anticancer agents,<sup>[7b]</sup> the antiproliferative activities of **2** were evaluated. To avoid possible bias from enantiopure compounds, selected racemic compounds were initially tested and are summarized in Table 4. In the screening, it was found that the racemic mixture of **2o** showed promising biological activity with an  $IC_{50}$  of approximately 2  $\mu$ M. Next, we examined each enantiomer of **2o**. While **2o** showed 2 to 3 times lower activity, retentive antiproliferative activity was observed with *ent*-**2o**. This result supports the importance of atroposelective methods for biologically relevant compounds.<sup>[20]</sup>

In conclusion, a new strategy for catalytic and highly atroposelective Pictet–Spengler reactions of *N*-arylindoles via DKR has been established. Chiral phosphoric acids smoothly led to cyclization to afford the highly enantioenriched *N*-aryl-tetrahydro- $\beta$ -carbolines about a stereogenic C–N bond axis. Application to benzaldehydes enables the control of both point and axial stereogenicity by securing more stereochemically complex molecules. The newly synthesized tetrahydro- $\beta$ -carbolines showed promising antiproliferative activity, which could lead to new and unique scaffolds for drug discovery.

**Table 4:** Anti-proliferative activities of **2**.<sup>[a,b]</sup>

Compd.	$IC_{50}$ ( $\mu$ M)			
	A549	MDA-MB-231	SK-Hep-1	SNU-638
( $\pm$ )- <b>2b</b>	11 $\pm$ 2.9	10 $\pm$ 3.1	11 $\pm$ 1.9	9.4 $\pm$ 2.6
( $\pm$ )- <b>2d</b>	> 50	> 50	> 50	> 50
( $\pm$ )- <b>2e</b>	23 $\pm$ 6.3	13 $\pm$ 3.3	13 $\pm$ 1.8	25 $\pm$ 4.1
( $\pm$ )- <b>2h</b>	12 $\pm$ 3.1	9.5 $\pm$ 1.9	10 $\pm$ 2.4	5.7 $\pm$ 0.94
( $\pm$ )- <b>2i</b>	3.4 $\pm$ 1.5	2.5 $\pm$ 0.78	2.6 $\pm$ 0.63	2.4 $\pm$ 1.1
( $\pm$ )- <b>2m</b>	11 $\pm$ 3.3	10 $\pm$ 2.8	12 $\pm$ 3.9	5.8 $\pm$ 1.7
( $\pm$ )- <b>2o</b>	2.6 $\pm$ 0.67	2.5 $\pm$ 0.69	2.5 $\pm$ 0.84	2.6 $\pm$ 0.88
( $\pm$ )- <b>2p</b>	2.6 $\pm$ 0.93	3.9 $\pm$ 1.3	2.6 $\pm$ 0.72	2.7 $\pm$ 0.91
Doxorubicin (nM)	24 $\pm$ 12	78 $\pm$ 16	98 $\pm$ 23	36 $\pm$ 17



[a] A549: Human lung cancer cell line; MDA-MB-231: Human breast cancer cell line; SK-Hep-1: Human liver cancer cell line; SNU-638: Human stomach cancer cell line. [b] Data are represented as means  $\pm$  SD. The results are representative of three independent experiments. Measured by the SRB method.<sup>[17]</sup>

## Acknowledgements

This work is supported by the National Research Foundation of Korea (NRF) grant funded by the Korea government (MSTI) (No. 2020R1C1C1006231)

## Conflict of interest

The authors declare no conflict of interest.

**Keywords:** atropisomerism · chiral phosphoric acid · C–N stereogenic axis · dynamic kinetic resolution · Pictet–Spengler cyclization

- [1] a) J. M. Lassaletta, *Atropisomerism and Axial Chirality*, World Scientific, New Jersey, **2019**; b) G. Bringmann, T. Gulder, T. A. M. Gulder, M. Breuning, *Chem. Rev.* **2011**, *111*, 563–639.
- [2] For recent examples, see: a) J.-Z. Wang, J. Zhou, C. Xu, H. Sun, L. Kürti, Q.-L. Xu, *J. Am. Chem. Soc.* **2016**, *138*, 5202–5205; b) O. Quinonero, M. Jean, N. Vanthuyne, C. Roussel, D. Bonne, T. Constantieux, C. Bressy, X. Bugaut, J. Rodriguez, *Angew. Chem. Int. Ed.* **2016**, *55*, 1401–1405; *Angew. Chem.* **2016**, *128*, 1423–1427; c) M. M. Cardenas, S. T. Toenjes, C. J. Nalbandian, J. L. Gustafson, *Org. Lett.* **2018**, *20*, 2037–2041; d) C. Zhao, D. Guo, K. Munkerup, K.-W. Huang, F. Li, J. Wang, *Nat. Commun.* **2018**, *9*, 611; e) J.-Y. Liu, X.-C. Yang, Z. Liu, Y.-C. Luo, H. Lu, Y.-C. Gu, R. Fang, P.-F. Xu, *Org. Lett.* **2019**, *21*, 5219–5224; f) S. Lu, S. V. H. Ng, K. Lovato, J.-Y. Ong, S. B. Poh, X. Q. Ng, L. Kürti, Y. Zhao, *Nat. Commun.* **2019**, *10*, 3061; g) S. Lu, J.-Y. Ong, H. Yang, S. B. Poh, X. Liew, C. S. D. Seow, M. W. Wong, Y. Zhao, *J. Am. Chem. Soc.* **2019**, *141*, 17062–17067; h) L. Peng, K. Li, C. Xie, S. Li, D. Xu, W. Qin, H. Yan, *Angew. Chem. Int. Ed.* **2019**, *58*, 17199–17204; *Angew. Chem.* **2019**, *131*, 17359–17364; i) R. M. Witzig, V. C. Fäseke, D. Häussinger, C. Sparr, *Nat. Catal.* **2019**, *2*, 925–930; j) K. Xu, W. Li, S. Zhu, T. Zhu, *Angew. Chem. Int. Ed.* **2019**, *58*, 17625–17630; *Angew. Chem.* **2019**, *131*, 17789–17794; k) C. Ma, F.-T. Sheng, H.-Q. Wang, S. Deng, Y.-C. Zhang, Y. Jiao, W. Tan, F. Shi, *J. Am. Chem. Soc.* **2020**, *142*, 15686–15696; l) A. Romero-Arenas, V. Hornillos, J. Iglesias-Sigüenza, R. Fernández, J. López-Serrano, A. Ros, J. M. Lassaletta, *J. Am. Chem. Soc.* **2020**, *142*, 2628–2639; m) G. Wang, Q. Shi, W. Hu, T. Chen, Y. Guo, Z. Hu, M. Gong, J. Guo, D. Wei, Z. Fu, W. Huang, *Nat. Commun.* **2020**, *11*, 946; n) C.-C. Xi, X.-J. Zhao, J.-M. Tian, Z.-M. Chen, K. Zhang, F.-M. Zhang, Y.-Q. Tu, J.-W. Dong, *Org. Lett.* **2020**, *22*, 4995–5000; o) B.-B. Zhan, L. Wang, J. Luo, X.-F. Lin, B.-F. Shi, *Angew. Chem. Int. Ed.* **2020**, *59*, 3568–3572; *Angew. Chem.* **2020**, *132*, 3596–3600; p) J. Zhang, M. Simon, C. Golz, M. Alcarazo, *Angew. Chem. Int. Ed.* **2020**, *59*, 5647–5650; *Angew. Chem.* **2020**, *132*, 5696–5699.
- [3] For reviews, see: a) I. Takahashi, Y. Suzuki, O. Kitagawa, *Org. Prep. Proced. Int.* **2014**, *46*, 1–23; b) D. Bonne, J. Rodriguez, *Chem. Commun.* **2017**, *53*, 12385–12393; c) V. Corti, G. Bertuzzi, *Synthesis* **2020**, *52*, 2450–2468.
- [4] For selected examples, see: a) L. Zhang, J. Zhang, J. Ma, D.-J. Cheng, B. Tan, *J. Am. Chem. Soc.* **2017**, *139*, 1714–1717; b) L. Zhang, S.-H. Xiang, J. Wang, J. Xiao, J.-Q. Wang, B. Tan, *Nat. Commun.* **2019**, *10*, 566; c) J. Zhang, Q. Xu, J. Wu, J. Fan, M. Xie, *Org. Lett.* **2019**, *21*, 6361–6365; d) J. Frey, A. Malekafzali, I. Delso, S. Choppin, F. Colobert, J. Wencel-Delord, *Angew. Chem. Int. Ed.* **2020**, *59*, 8844–8848; *Angew. Chem.* **2020**, *132*, 8929–8933; e) N. Man, Z. Lou, Y. Li, H. Yang, Y. Zhao, H. Fu, *Org. Lett.* **2020**, *22*, 6382–6387; f) W. Xia, Q.-J. An, S.-H. Xiang, S. Li, Y.-B. Wang, B. Tan, *Angew. Chem. Int. Ed.* **2020**, *59*, 6775–6779; *Angew. Chem.* **2020**, *132*, 6841–6845; g) C.-X. Ye, S. Chen, F. Han, X. Xie, S. Ivlev, K. N. Houk, E. Meggers, *Angew. Chem. Int. Ed.* **2020**, *59*, 13552–13556; *Angew. Chem.* **2020**, *132*, 13654–13658.
- [5] a) J. A. Joule, K. Mills, *Heterocyclic Chemistry*, Blackwell Science Oxford, **2000**; b) T. Eicher, S. Hauptmann, A. Speicher, *The Chemistry of Heterocycles*, Wiley-VCH, Weinheim, **2003**.

- [6] a) J. Dai, W. Dan, U. Schneider, J. Wang, *Eur. J. Med. Chem.* **2018**, *157*, 622–656; b) M. Ozawa, Y. Nakada, K. Sugimachi, F. Yabuuchi, T. Akai, E. Mizuta, S. Kuno, M. Yamaguchi, *Jpn. J. Pharmacol.* **1994**, *64*, 179–188; c) E. Schlittler, A. Furlenmeier, *Helv. Chim. Acta* **1953**, *36*, 2017–2020.
- [7] a) M. Milen, P. Ábrányi-Balogh, *Chem. Heterocycl. Compd.* **2016**, *52*, 996–998; b) S. Kumar, A. Singh, K. Kumar, V. Kumar, *Eur. J. Med. Chem.* **2017**, *142*, 48–73.
- [8] a) Y. Wang, P. Zhang, X. Di, Q. Dai, Z.-M. Zhang, J. Zhang, *Angew. Chem. Int. Ed.* **2017**, *56*, 15905–15909; *Angew. Chem.* **2017**, *129*, 16121–16125; b) G. Cera, M. Lanzi, D. Balestri, N. Della Ca, R. Maggi, F. Bigi, M. Malacria, G. Maestri, *Org. Lett.* **2018**, *20*, 3220–3224.
- [9] a) A. Pictet, T. Spengler, *Ber. Dtsch. Chem. Ges.* **1911**, *44*, 2030–2036; b) G. Tatsui, *J. Pharm. Soc. Jpn.* **1928**, *48*, 453–459.
- [10] R. Dalpozzo, *Molecules* **2016**, *21*, 699.
- [11] J. Seayad, A. M. Seayad, B. List, *J. Am. Chem. Soc.* **2006**, *128*, 1086–1087.
- [12] a) R. S. Klausen, E. N. Jacobsen, *Org. Lett.* **2009**, *11*, 887–890; b) R. S. Klausen, C. R. Kennedy, A. M. Hyde, E. N. Jacobsen, *J. Am. Chem. Soc.* **2017**, *139*, 12299–12309; c) C. Zhao, S. B. Chen, D. Seidel, *J. Am. Chem. Soc.* **2016**, *138*, 9053–9056; d) E. Mons, M. J. Wanner, S. Ingemann, J. H. van Maarseveen, H. Hiemstra, *J. Org. Chem.* **2014**, *79*, 7380–7390; e) C. L. Hansen, R. G. Ohm, L. B. Olsen, E. Ascic, D. Tanner, T. E. Nielsen, *Org. Lett.* **2016**, *18*, 5990–5993; f) S. Das, L. Liu, Y. Zheng, M. W. Alachraf, W. Thiel, C. K. De, B. List, *J. Am. Chem. Soc.* **2016**, *138*, 9429–9432; g) S.-G. Wang, Z.-L. Xia, R.-Q. Xu, X.-J. Liu, C. Zheng, S.-L. You, *Angew. Chem. Int. Ed.* **2017**, *56*, 7440–7443; *Angew. Chem.* **2017**, *129*, 7548–7551; h) N. Glinsky-Olivier, S. Yang, P. Retailleau, V. Gandon, X. Guinchard, *Org. Lett.* **2019**, *21*, 9446–9451; i) R. Andres, Q. Wang, J. Zhu, *J. Am. Chem. Soc.* **2020**, *142*, 14276–14285; j) A. Nalikezhathu, V. Cherepakhin, T. J. Williams, *Org. Lett.* **2020**, *22*, 4979–4984; k) Z. Zhu, M. Odagi, C. Zhao, K. A. Abboud, H. U. Kirm, J. Saame, M. Lökov, I. Leito, D. Seidel, *Angew. Chem. Int. Ed.* **2020**, *59*, 2028–2032; *Angew. Chem.* **2020**, *132*, 2044–2048.
- [13] a) T. Akiyama, J. Itoh, K. Yokota, K. Fuchibe, *Angew. Chem. Int. Ed.* **2004**, *43*, 1566–1568; *Angew. Chem.* **2004**, *116*, 1592–1594; b) D. Uruguchi, M. Terada, *J. Am. Chem. Soc.* **2004**, *126*, 5356–5357.
- [14] a) A. Zamfir, S. Schenker, M. Freund, S. B. Tsogoeva, *Org. Biomol. Chem.* **2010**, *8*, 5262–5276; b) S. Schenker, A. Zamfir, M. Freund, S. B. Tsogoeva, *Eur. J. Org. Chem.* **2011**, 2209–2222; c) D. Parmar, E. Sugiono, S. Raja, M. Rueping, *Chem. Rev.* **2014**, *114*, 9047–9153; d) F. E. Held, D. Grau, S. B. Tsogoeva, *Molecules* **2015**, *20*, 16103–16126; e) R. Maji, S. C. Mallojjala, S. E. Wheeler, *Chem. Soc. Rev.* **2018**, *47*, 1142–1158.
- [15] a) J. L. Gustafson, D. Lim, S. J. Miller, *Science* **2010**, *328*, 1251–1255; b) K. Mori, T. Itakura, T. Akiyama, *Angew. Chem. Int. Ed.* **2016**, *55*, 11642–11646; *Angew. Chem.* **2016**, *128*, 11814–11818.
- [16] a) C. He, M. Hou, Z. Zhu, Z. Gu, *ACS Catal.* **2017**, *7*, 5316–5320; b) C. Ma, F. Jiang, F.-T. Sheng, Y. Jiao, G.-J. Mei, F. Shi, *Angew. Chem. Int. Ed.* **2019**, *58*, 3014–3020; *Angew. Chem.* **2019**, *131*, 3046–3052; c) F. Jiang, K.-W. Chen, P. Wu, Y.-C. Zhang, Y. Jiao, F. Shi, *Angew. Chem. Int. Ed.* **2019**, *58*, 15104–15110; *Angew. Chem.* **2019**, *131*, 15248–15254.
- [17] See the Supporting Information for details.
- [18] W.-D. Chu, Y. Zhang, J. Wang, *Catal. Sci. Technol.* **2017**, *7*, 4570–4579.
- [19] In the absence of **P9**, the reaction of **1b** and paraformaldehyde in toluene (0.050 mmol of **1b**, 0.075 mmol of paraformaldehyde, 0.5 mL of toluene, 23 h, and 2 °C) provided **2b** in 94% yield.
- [20] a) S. R. LaPlante, L. D. Fader, K. R. Fandrick, D. R. Fandrick, O. Huckle, R. Kemper, S. P. F. Miller, P. J. Edwards, *J. Med. Chem.* **2011**, *54*, 7005–7022; b) P. W. Glunz, *Bioorg. Med. Chem. Lett.* **2018**, *28*, 53–60.

Manuscript received: January 9, 2021

Revised manuscript received: February 16, 2021

Accepted manuscript online: March 2, 2021

Version of record online: April 23, 2021